The SH3 domains of the protein kinases ITK and LCK compete for adjacent sites on T cell-specific adapter protein

Thorny Cesilie Bie Andersen[1], Per Eugen Kristiansen[2], Zsuzsa Huszenicza[1], Maria U. Johansson[3], Ramakrishna Prabhu Gopalakrishnan[1], Hanna Kjelstrup[1], Scott Boyken[4], Vibeke Sundvold-Gjerstad[1], Stine Granum[1], Morten Sørli[5], Paul Hoff Backe[6,7], D. Bruce Fulton[4], B. Göran Karlsson[3], Amy H. Andreotti[4], and Anne Spurkland[1*]

[1] From the Institute of Basic Medical Sciences, Department of Molecular Medicine, University of Oslo, Norway; [2]Department of Biosciences, University of Oslo, Norway; [3] The Swedish NMR Centre at University of Gothenburg, Gothenburg, Sweden; [4]The Roy J. Carver Department of Biochemistry, Biophysics and Molecular Biology, Iowa State University, Ames, IA USA; [5]Department of Chemistry, Biotechnology and Food Science, The Norwegian University of Life Sciences, Ås, Norway; [6]Department of Microbiology, Oslo University Hospital and University of Oslo, Oslo, Norway; [7]Department of Medical Biochemistry, Oslo University Hospital and University of Oslo, Oslo, Norway

Running title: *ITK SH3-interaction with TSAD*

*To whom correspondence should be addressed: Anne Spurkland, Institute of Basic Medical Sciences, University of Oslo, Pb 1105 Blindern, 0317 Oslo, Norway. Phone +4722851125; Fax: +4722861278; E-mail: anne.spurkland@medisin.uio.no

Keywords: cell **signaling**, SRC homology 3 domain, tyrosine-protein kinase, nuclear magnetic resonance (NMR), protein-protein interaction, SH2D2A, LCK proto-oncogene SRC family tyrosine kinase (LCK), IL-2–inducible T cell kinase (ITK), T cell–specific adapter protein (TSAD), immunity

ABSTRACT

T-cell activation requires stimulation of specific intracellular signaling pathways in which protein tyrosine kinases, phosphatases, and adapter proteins interact to transmit signals from the T-cell receptor to the nucleus. Interactions of LCK proto-oncogene, SRC family tyrosine kinase (LCK)[1] and the IL-2–inducible T cell kinase (ITK) with the T cell-specific adapter protein (TSAD) promotes LCK-mediated phosphorylation and thereby ITK activation. Both ITK and LCK interact with TSAD's proline rich region (PRR) through their SH3 domains. Whereas LCK may also interact with TSAD through its SH2 domain, ITK interacts with TSAD only through its SH3 domain. To begin to understand on a molecular level how the LCK SH3 and ITK SH3 domains interact with TSAD in human HEK293T cells, here we combined biochemical analyses with NMR spectroscopy. We found that the ITK- and LCK-SH3 domains potentially have adjacent and overlapping binding sites within the TSAD PRR amino acids (aa)239–274. Pull-down experiments and NMR spectroscopy revealed that both domains may bind to TSAD aa239–256 and aa257–274. Co-immunoprecipitation experiments further revealed that both domains may also bind simultaneously to TSAD aa242-268. Accordingly, NMR spectroscopy indicated that the SH3 domains may compete for these two adjacent binding sites. We propose that once the associations of ITK and LCK with TSAD promote the ITK and LCK interaction, the interactions among TSAD, ITK and LCK are dynamically altered by ITK phosphorylation status.

T cell activation relies upon stimulation of specific intra cellular signal-transduction pathways, where protein tyrosine kinases (PTKs), phosphatases and adapter molecules interact to convey the signal from the T cell receptor (TCR) to the nucleus. Adapter molecules present

specific protein interaction sites, but lack intrinsic enzymatic activity (1). These molecules bridge interactions between other proteins in the signaling cascade, such as the PTKs and their substrates. PTKs in T cells include at least four families: the Src family, the SYK family, the CSK family and the TEC family (2). The TEC family IL-2 Inducible tyrosine kinase (ITK) is recruited to the membrane after TCR triggering, and is activated by the SRC family PTK Lymphocyte specific kinase (LCK). This results in activation of phospholipase C gamma 1 (PLCγ1), eventually leading to gene transcription via intracellular Ca^{2+} release and transcription factor activation (reviewed in (3)).

The T cell specific adapter protein (TSAD), encoded by the *SH2D2A* gene, is an adapter molecule containing a SRC homology 2 (SH2) domain and a proline rich region (PRR) in addition to several tyrosine phosphorylation sites (4,5). The gene was first isolated from an activated CD8+ T cell cDNA library by differential screening (4), and was later identified as an interaction partner to other signaling molecules, including LCK (6) and ITK (7).

TSAD influences T cell signaling via its interaction with the tyrosine kinases LCK and ITK (8). Both ITK and TSAD are expressed at low levels in naïve T cells, but are induced upon activation of T cells (4,9,10). Absence of TSAD results in deficient polarization of actin to the immunological synapse (8), as well as deficient activation induced cell death (11).

Both LCK and ITK consist of multiple domains, including one SH2 and one SRC homology 3 (SH3) domain (12). SH3 domains are regions of approximately 60–70 amino acids (aa) present in many signaling molecules. The general structure of this domain consists of two short anti-parallel β-sheets packed against each other, resulting in a fold with a relatively flat hydrophobic surface containing at least one conserved aromatic (often a tryptophan) residue (13). SH3 domains bind to PRRs that can contain the prototypic SH3-binding motif PxxP belonging to one of two classes. Class I motifs have the consensus sequence +pΨPpΨP, class II have the consensus sequence ΨPpΨPp+. Ψ represents aliphatic residues, + indicates basic residues, uppercase positions are conserved residues which contact the SH3 domain and provides the specificity, and lower case residues represents scaffolding positions, usually prolines (14). Ligand orientation is generally determined by the position of the basic residue, often an arginine, relative to the core proline residues (15).

We have previously mapped the interaction site of ITK on TSAD, and showed that ITK binds with its SH3 domain to the PRR of TSAD (aa239–274) (10), in a region coincident with that of LCK SH3 interacting with TSAD (16). Interaction of TSAD with ITK promoted LCK mediated tyrosine phosphorylation of ITK, as well as migration of T cells upon CXCL12 stimulation. T cells lacking TSAD failed to induce tyrosine phosphorylation of ITK, as well as migration of T cells upon CXCL12 stimulation (10). While ITK interacts with TSAD exclusively through its SH3 domain (10), LCK interacts with TSAD through both its SH3 and its SH2 domain (17). Thus, promotion of LCK-mediated phosphorylation of ITK by TSAD could be either due to simultaneous docking and interaction of LCK and ITK on TSAD, or simply that binding of LCK to TSAD activates LCK catalytic activity, thus facilitating phosphorylation of ITK.

In an effort to begin to understand the molecular details defining the association of TSAD, LCK and ITK, we performed peptide array binding experiments, biochemical analyses and 2D (^{1}H, ^{15}N) heteronuclear single quantum coherence (HSQC) NMR experiments to examine the interaction between TSAD, ITK SH3 and LCK SH3. Our data support a model whereby LCK and ITK are both recruited to TSAD via their SH3 domains, allowing LCK mediated phosphorylation of ITK. Our results point to a complex protein assembly, where the ITK-SH3 and LCK-SH3 domains can both compete for and simultaneously bind to adjacent binding sites on TSAD encompassing aa242–268. Our findings also suggest that, once active, ITK autophosphorylation of its own SH3 domain disrupts the ITK/TSAD interaction, possibly creating an open binding site on TSAD for recruiting and activation of another ITK molecule by LCK.

Results

Interaction of TSAD with ITK is dependent on the intact ITK-SH3 domain

Expression of the adapter molecule TSAD (Fig. 1*A*) is induced in human T-cells upon TCR-triggering (9) concomitant with ITK (10). Murine TSAD was first cloned as an ITK/RLK interaction partner, thus an alternative designation for TSAD is RLK/ITK binding protein (RIBP) (7). Following up on this observation, we have previously found that the interaction of TSAD with ITK is dependent on the PRR of TSAD (10), indicating a role for the ITK-SH3 domain in mediating this interaction. To reveal whether an intact ITK-SH3 domain is required for interaction of ITK with TSAD, we expressed full length myc-tagged ITK constructs in 293T cells, and performed co-immunoprecipitation experiments. Immunoprecipitation of ITK led to co-immunoprecipitation of TSAD only in the presence of wild type ITK, while ITK containing the W208K mutation, which is known to abolish binding of ITK-SH3 domain to its ligands (18), did not co-immunoprecipitate with TSAD (Fig. 1*B*).

We previously also showed that TSAD promotes LCK mediated phosphorylation of ITK on Tyr^{511} (10). This phosphorylation event activates the ITK kinase and leads to auto phosphorylation of ITK Tyr^{180} in the ITK-SH3 domain (19). It has been shown that the specificity of ITK SH3 for its ligands may be altered by Tyr^{180} phosphorylation (20). In order to examine whether binding of ITK SH3 to TSAD was affected by phosphorylation of ITK Tyr^{180}, we generated Y-F and Y-E mutated versions of the ITK-SH3 domain.

Both the ITK-SH3 Y180F and the Y180E mutant proteins displayed significantly reduced interaction with TSAD compared to the wild type ITK-SH3 domain (Fig. 1*C* and *D*). Also compared to the ITK-SH3 Y180F mutant, the Y180E mutant, where the negative charge and the size of the glutamate in the ITK-Y180E mutant may mimic ITK phosphor (p)Tyr^{180}, displayed significantly reduced binding to TSAD (Fig. 1*D*).

Taken together, these data show that interaction of TSAD with ITK is mediated by ITK SH3, furthermore it suggests that the physiological association between the two molecules is regulated by the phosphorylation status of ITK.

LCK SH3 and ITK SH3 bind to overlapping peptides in TSAD PRR

Having established that ITK SH3 binds to TSAD, we performed *in silico* motif analysis (http://scansite.mit.edu/) (21) using the human TSAD amino acid sequence as input (Genbank: Q9NP31) and the default matrix for ITK-SH3 ligands. This analysis revealed possible ITK-SH3 binding sites at TSAD Pro^{263} and Pro^{247} (Fig. 2*A*). TSAD Pro^{247} was also indicated as a potential SRC-SH3 interaction site (data not shown). We then went on to dissect the interaction between the ITK-SH3 domain and the PRR of TSAD compared to that of the LCK-SH3 domain, which is known to bind to TSAD (17). A series of 14 overlapping peptides of 20 aa with a sliding window of three aa was synthesized and fixed onto a cellulose membrane. This peptide array covered most of the PRR of TSAD (aa233–291) (Fig. 2*B*). The membrane was probed with recombinant GST-ITK-SH3 and GST-LCK-SH3 domains, and immunoblotted with anti-GST and anti-mouse-HRP antibodies. The results show that ITK-SH3 and LCK-SH3 domains bind to overlapping peptides in the PRR of TSAD. However, the peptide array blotting analysis indicates that ITK SH3 prefers a binding site that is C-terminal relative to that preferred by LCK SH3 (Fig. 2*A*). The mutant ITK-SH3 domain W208K (ITK-K), did not bind to any of the TSAD peptides.

The ITK SH3 binding motif in TSAD PRR is focused on Pro^{263}

The motif formed by the TSAD sequence flanking Pro^{263} (**P**ΨPXXRP) is also found in the ITK-SH3 binding motifs of SLP-76 and in CBL-B (18,22,23) as well as putative ITK-SH3 ligands as predicted by Scansite (Table 1). Mutation of either of Pro^{247} or Pro^{263} to alanines did not significantly abolish binding of ITK SH3 to TSAD in pull-down experiments (Fig. 2*C* and *D*), indicating that more than one amino acid in these regions are involved in binding to the ITK-SH3 domain. Consistent with the presence of two ITK-SH3 interaction sites on TSAD within aa239–273 (Fig. 2*A* and *B*) we found that a deletion mutant of TSAD lacking both the Pro^{247} and the Pro^{263} motifs (TSAD Δ239–274) displayed minimal binding to ITK SH3 (Fig. *2E*

lane 3 and Fig. 2*F*) as has previously been shown (10). In contrast separate deletion constructs encompassing either Pro^{247} or Pro^{263}, TSAD Δ239–256 and TSAD Δ257–274 respectively, both retained some binding to ITK SH3 (Fig. 1*A* and Fig. 2*E*, lane 4 and 5). The deletion construct lacking Pro^{263} (TSAD Δ257–274) showed a significantly greater reduction in binding ITK SH3 compared to TSAD Δ239–256 (Fig. 2*F*).

The observation that neither of the two shorter deletions completely eliminated ITK-SH3 interaction, indicated that the continued presence of the remaining Pro^{247} or Pro^{263} motives were sufficient for ITK-SH3 interaction. Mutation of Pro^{263} to Ala^{263} in TSAD Δ239–256 resulted in significantly reduced interaction of ITK SH3 with TSAD. Also the corresponding Pro^{247} to Ala^{247} mutation in TSAD Δ257–274 conferred reduced interaction with ITK SH3, however, the difference failed to reach statistical significance (Fig 2*G* and *H*).

Taken together, we therefore hypothesized that the interaction of TSAD Pro^{263} with ITK SH3 was the most likely to be of biological relevance, and hence set out to analyze this interaction in further detail using NMR spectroscopy.

The human ITK-SH3 domain binds to TSAD aa262–269 in a class I orientation

We determined the NMR resonance assignments (deposited as BMRBid: 18119) and three-dimensional structure of the human ITK-SH3 domain (PDBid: 2LMJ) using standard methods (24). The structures are shown in Fig. 3 and the structure statistics in Table 2. The obtained structure showed an SH3 structure similar to that of murine ITK SH3 (PDBid:2RNA) (25). Similarly, no major differences are observed between this structure and the NMR structure of human ITK SH3 determined by the RIKEN structural genomics initiative (PDBid: 2YUQ).

A series of 2D ^{1}H-^{15}N HSQC experiments were recorded after titration of increasing amounts of TSAD peptide. The peptide *IPVPRHRPAPRPKPSNP# (aa262-278) was chosen for analysis since it contains both a partial class II motif including Pro^{263} and a class I motif (15) corresponding to the consensus sequences PxxPx[RK] and [RK]xxPxxP respectively. N-terminal and C-terminally truncated versions of the peptide (aa262–269 (*IPVPRHRP#) containing the partial class II motif and aa 271-278 (*PRPKPSNP#) containing the class I motif) were also analysed. The chemical shift changes that occurred upon ligand binding to the N-terminal peptide aa262-269 (Fig. 4*A*) indicate SH3 residues that were affected by ligand binding. The longer aa262–278 peptide gave similar shifts as the aa262–269 peptide, while the aa271–278 peptide did not induce chemical shift changes (data not shown). The chemical shift changes induced upon binding of TSAD aa262–269 as well as TSAD aa262–278 mapped within the conventional binding surface of SH3 domains (13) onto the structure of the human ITK SH3 (data not shown). These data did not, however, reveal information about the orientation of the peptide binding to ITK SH3.

In order to map the binding orientation of the peptide, we used a custom made spin-labeled peptide containing a helicogenic nitroxyl aa (*i.e.* TOAC) at its N terminus. The TOAC aa in the bound peptide will influence the chemical environment of the ITK-SH3 domain upon peptide binding and cause broadening of peaks in the NMR spectrum corresponding to aa in proximity of the spin-label. Comparison of ^{1}H-^{15}N-HSQC spectra of 500 μM ^{15}N-labeled recombinant human ITK-SH3 domain alone and in complex with 1 mM TOAC-peptide revealed that the TOAC label most strongly affected the peaks corresponding to Leu^{201}, Trp^{208}, Arg^{214} and Val^{176}, with a 25–35% reduction in peak volumes (Fig. 4*B*). These data indicate that binding of the TSAD peptide to ITK SH3 brings the N-terminal TOAC moiety close to these aa, which all are located in the vicinity of the specificity pocket of human ITK-SH3 domain. Based on our data, we thus modeled the TSAD peptide bound to ITK SH3 with the N-terminal pointing towards the specificity pocket by application of HADDOCK (26). The model of the TOAC-labeled TSAD peptide bound to ITK SH3 is shown in Fig. 4*C*. Taken together, our data indicate that the binding orientation of the TSAD peptide aa262–269 on human ITK SH3 is in a class I orientation (15) with the N-terminal end of the peptide ligand pointing towards the specificity pocket.

Both LCK SH3 and ITK SH3 may bind simultaneously to the TSAD PRR

Since LCK SH3 and ITK SH3 bind to overlapping peptides in the TSAD PRR (Fig. 2*A*) and ITK-SH3 domain binds to the TSAD aa262–269 peptide (Fig. 4), we directly assessed whether LCK SH3 and ITK SH3 may bind to adjacent sites on the same TSAD peptide. We first performed pull down of TSAD deletion mutants using GST-LCK-SH3 as a bait (Fig. 5*A*-*C*). The results showed that while TSAD Δ239–274 essentially abolished interaction of LCK SH3 with TSAD, both the two shorter deletions (TSAD Δ239–256 or Δ257–274) retained some binding to TSAD (Fig. 5*A* and *C*). Mutation of Pro^{263} to Ala^{263} in TSAD Δ239–256 significantly reduced interaction of LCK SH3 further, while the mutation Pro^{247} to Ala^{247} in TSAD Δ257–274 did not significantly reduce interaction with LCK SH3 (Fig. 5*B* and *C*).

To further substantiate that LCK SH3 and ITK SH3 both bind to adjacent sites in the TSAD PRR, a 27 amino acid peptide representing TSAD aa242–268
(*LLRPKPPIPAKPQLPPEVYTIPVPRHR#)
and two shorter peptides derived from TSAD aa242–258 and aa254-268 were synthesized (Fig. *1A* and 5*D*). An *in vitro* pull-down experiment using an equimolar mixture of GST-ITK-SH3 (bound to glutathione Sepharose™ beads) with soluble HA-tagged LCK-SH3 in the absence or the presence of increasing amounts of the TSAD aa242–268 peptide was then performed. The result showed that GST-ITK-SH3 associated with HA-LCK-SH3 only in the presence of TSAD aa242–268 (Fig. 5*E*). Moreover, increasing the concentration of TSAD aa242–268 in the pull-down assay resulted in decreased association of HA-LCK-SH3 with GST-ITK-SH3 (Fig. 5*E*). This latter finding suggests that at higher concentrations of TSAD peptide, binary SH3/peptide complexes are favored over a ternary complex containing TSAD and two SH3 domains. We also found that only the long peptide (TSAD aa242–268) facilitates association between the ITK and LCK-SH3 domains, as identical pull-down experiments using the two shorter TSAD peptides (aa242–258 and aa254-268) resulted in no detectable association between GST-ITK-SH3 and HA-LCK-SH3 (Fig. 5*F*).

ITK SH3 competes with LCK SH3 for binding to TSAD PRR

To further assess the association between TSAD and the ITK and LCK-SH3 domains we introduced both SH3 domains into the same NMR experiment. The ^{15}N labeled LCK-SH3 domain was first titrated with TSAD aa242–268 (Fig. 6*A*). A subset of resonances showed chemical shift perturbations consistent with binding of the TSAD peptide to the LCK-SH3 domain. Next, the unlabeled ITK-SH3 domain was added to the 1:2 LCK SH3/TSAD peptide mixture in the NMR tube. For all LCK SH3 resonances that shifted upon addition of TSAD aa242–268, we observed resonance changes in the direction of unbound LCK SH3 (Fig. 6*A* and *B*). Moreover, we did not detect chemical shift changes in the LCK-SH3 domain outside of the peptide binding pocket upon addition of ITK SH3 suggesting a lack of interaction between the LCK and ITK-SH3 domains themselves (data not shown). When we performed the experiment in the reverse order, using ^{15}N labeled ITK-SH3 domain titrated with TSAD aa242–268, and added unlabeled LCK-SH3 domain to the 1:2 ITK SH3/TSAD peptide mixture in the NMR tube, similar results were obtained (data not shown).

Taken together, our data presented in Fig. 2 and 5 suggest that ITK SH3 as well as LCK SH3 may each have two adjacent binding sites on TSAD. To further examine this notion, using NMR spectroscopy, we titrated an equimolar mixture of the two ^{15}N labeled isolated SH3 domains with either of the two shorter TSAD derived peptides aa242–258 and aa254-268. Both SH3 domains displayed resonances that shifted upon addition of both peptides, representing amino acids located to the peptide binding surface of the SH3 domain (Fig. 6*C*). Each of the LCK SH3 or ITK SH3 resonances that shifted upon addition of the peptides, shifted in different directions depending on the identity of the peptide (Fig. 6*C*), indicating that the chemical environment provided by the two peptides were indeed different. These results show that both SH3 domains may bind to two adjacent ligands contained within TSAD aa242–268.

Finally we characterized the binding of ITK SH3 and LCK SH3 with the TSAD PRR. Using the NMR titration data shown in Fig. 6*C* where both SH3 domains were present in equimolar amounts as well as similar titrations using TSAD aa242–268 (not shown), we assessed the relative affinities of the different regions of the TSAD PRR for the ITK and LCK-SH3 domains. TSAD aa242–268 spanning the PRR, bound equally well *in vitro* to both ITK and LCK-SH3 domains (Table 3, Fig. 6*D*). TSAD aa242–258, the N-terminal region of the PRR, also bound to both ITK- and LCK-SH3 domains (Table 3, Fig. 6*D*). The dissociation constants for TSAD aa242–268, and the N-terminal half of the same peptide, TSAD aa242–256, were similar (Table 3), suggesting that most of the *in vitro* binding between the SH3 domains and the TSAD peptide is mediated by the aa stretch between residues 242 and 256. This was further supported by titrations using TSAD aa254–268 representing the C-terminal half of the TSAD peptide. Chemical shift changes that resulted from titration of this peptide did not approach saturation within the range of concentrations tested (Fig. 6*D*). Thus, in this NMR titration experiment, the N-terminal half of the TSAD PRR appears to contain the preferred binding site for both ITK and LCK-SH3 domains.

The TSAD aa239–274 sequence is required for LCK mediated phosphorylation of ITK

Taken together, our data point to a model for the LCK, TSAD, ITK signaling system that involves binding of both kinases to the TSAD scaffold, to facilitate LCK mediated activation of ITK. Both the peptide array data (Fig. 2*A*), the mutagenesis and deletions within the TSAD sequence (Fig. 2*E* and *F* and Fig. 5*A*-*C*) as well as the NMR titration experiments suggest that the longer stretch of TSAD that includes Pro^{263} (TSAD aa242–268) is involved in association with LCK and ITK.

To directly assess whether the longer stretch of TSAD is required for LCK mediated phosphorylation of ITK, we transfected plasmids encoding the intact and truncated versions of TSAD together with LCK and myc-tagged ITK into 293T cells, and assessed the amount of ITK tyrosine phosphorylation. The results showed that in the absence of the PRR encoded by the aa239–274, TSAD does not promote phosphorylation of ITK (Fig. 7*A*). However, when either aa239–256 or aa257–274 is present in TSAD, a 50% reduction in the phosphorylation of ITK is observed compared to that observed in the presence of intact TSAD (Fig. 7*A* and *B*). This result indicates that both SH3 binding sites on TSAD contribute to the adapter function of TSAD, although the presence of both is not strictly required for TSAD to fulfill its role as a scaffold for LCK and ITK interaction.

ITK Tyr^{180} affects phosphorylation of ITK-Tyr^{511} as well as ITK association with TSAD

We then assessed the role of the auto-phosphorylation site ITK Tyr^{180} for LCK-mediated phosphorylation of ITK. As we had found that the Y180E mutant ITK SH3 domain mimicking ITK-$pTyr^{180}$, displayed reduced interaction with TSAD (Fig. 1*C*), we speculated that failure to phosphorylate ITK on Tyr^{180} would influence the dynamics of the TSAD-ITK interaction and thus phosphorylation of ITK by LCK on Tyr^{511} followed by autophosphorylation on Tyr^{180}. To assess to what extent the ITK-pTyr signal we observed in Fig. 7*A* represented either of these two tyrosines, we repeated the experiment shown in Fig. 7A lane 1 and 2, with a myc-ITK-Y180F mutant. The results showed that myc-ITK-Y180F displayed significantly reduced phosphorylation of ITK (Fig. 7*C* and *D*). This could be explained by much of the ITK phospho-Tyr signal observed using a pan-pTyr antibody as being contributed by ITK $pTyr^{180.}$ Some of the reduced signal could also be attributed to reduced interaction of the ITK-Y180F mutant with TSAD (Fig. 1*C* and *D* as well as Fig. 7*C*).

To distinguish between these two possibilities, we immunoprecipitated ITK from cells expressing myc-ITK or myc-ITK-Y180F in the presence of LCK and TSAD and directly assessed the total amount of ITK $pTyr^{511}$ using a phospho-site specific antibody. The result showed that in the absence of the autophosphorylation site Tyr^{180}, ITK was also less phosphorylated on Tyr^{511} (Fig 7*E* and *F*). This indicates that in the presence of TSAD, auto-phosphorylation of ITK Tyr^{180} is required for maximal phosphorylation of ITK Tyr^{511}. Reduced

binding ability of ITK pTyr^{180} to TSAD PRR, as indicated by our initial pull-down experiments using the phosphotyrosine mimic ITK Y180E SH3 domain (Fig 1*C* and *D*), may ensure that only non-phosphorylated ITK associates with TSAD once the TSAD PRR is accessible for binding. An additional consequence of this model could be that ITK that cannot be phosphorylated on Tyr^{180} will occupy TSAD PRR to a larger extent than wild type ITK, since an ITK molecule that is already bound to TSAD may immediately reassociate once it dissociates from the TSAD PRR. To test this assumption, we therefore immunoprecipitated TSAD from cells expressing either myc-ITK or myc-ITK-Y180F in the presence of TSAD and LCK, and probed for co-immunoprecipitation of ITK. This experiment revealed that more ITK Y180F than wild type ITK was associated to TSAD (Fig. 7*G* and *H*). Taken together, these data show that ITK Tyr^{180} regulates association of ITK to TSAD, and thereby also the phosphorylation of ITK Tyr^{511} by LCK.

Discussion

The adapter TSAD has multiple interaction sites and thus provides a platform for complex multi-modular protein-protein interactions within the T cell. We have previously mapped in detail how TSAD interacts with LCK (16), and have provided evidence that TSAD promotes LCK mediated phosphorylation of ITK on Tyr^{511} (10) in the activation loop of the kinase domain, a phosphorylation event that is critical for activation of ITK. In our present study we have begun to delineate the mode of interaction between TSAD and ITK. We show that TSAD may serve as a scaffold whereby ITK and LCK are brought into the vicinity of one another in the T cell. We propose that this LCK-ITK adapter function of TSAD promotes signaling downstream of ITK. A schematic overview of our model for how LCK and ITK interacts with TSAD is shown in Fig. 8.

In the current study, the biochemical analysis of the TSAD ITK LCK interactions was done exclusively in a heterologous cell system. The human embryonic kidney 293 (known as HEK293) cells, also expressing the SV40 large T antigen (known as 293T cells (27)) are commonly used for dissection of molecular mechanisms by exogenous expression of proteins. These cells have several advantages. While LCK is constitutively expressed in T cells, both ITK and TSAD are expressed only at low to moderate levels in resting or non-stimulated T cells and T cell lines. An additional advantage in using 293T cells for protein expression in eukaryotic cells, is that these cells do not express other T cell specific molecules that might interfere with the intermolecular interactions studied here. However, the stoichiometry and/or concentration of the interaction partners studied in 293T cells, may differ from the situation in actual T cells. For instance, while the interactions between TSAD, LCK and ITK appear to be independent of external, activating signals in 293T cells, this may not be the case at physiological conditions in T cells.

Our main finding in this study is that the ITK- and LCK-SH3 domains bind to adjacent sites on TSAD. Although they may both bind to TSAD at the same time, they also may compete for binding to the same site(s). LCK can bind to the three C-terminal TSAD tyrosines Tyr^{280}, Tyr^{290} and Tyr^{305} via its SH2 domain. The TSAD PRR interacting with LCK SH3 strongly promotes phosphorylation of these tyrosines (16). Thus, it is possible that LCK and ITK interact with TSAD sequentially, with LCK binding to TSAD first through its SH3 domain (Fig. 8A), and subsequently—after having phosphorylated the three C-terminal TSAD tyrosines—via its SH2 domain (Fig. 8B) leaving the PRR free to bind for ITK SH3 (Fig. 8C). This mechanism is consistent with the observations from NMR indicating direct competition between the SH3 domains for binding to the two shorter peptides representing the N- and the C-terminal parts of the TSAD PRR.

An increasing body of evidence suggests that within the cell, signaling molecules may form large complexes with multiple copies of each interacting partner (*i.e.* signalosomes) (28,29). The stoichiometric arrangement of ITK, LCK and TSAD in the cell may therefore be quite complex as has been suggested for the Grb2/LAT/SOS1 signaling system (30,31). The cell interior is virtually packed with molecules, probably resulting in localized regions with comparably high concentrations of given molecules (32). It is

increasingly being recognized that phase separation of signaling molecules may be functionally relevant (33). Thus the relatively high dissociation constants measured in the NMR tube with both SH3 domains present in high and equimolar concentrations, may still reflect physiologically meaningful molecular associations in the immediate vicinity of TSAD within the cell.

Once ITK is activated by LCK through phosphorylation of the Tyr^{511} (Fig. 8*D*) ITK auto phosphorylates Tyr^{180} in its own SH3 domain in cis (19,20). Moreover, autophosphorylation of ITK Tyr^{180} is required for full activity of ITK (19). Our findings suggest that autophosphorylation of the ITK SH3 domain in cis, results in the release of ITK from the TSAD scaffold (Fig. 8*E*). This creates an open binding site on TSAD for recruiting and activation of another ITK molecule by LCK (Fig. 8*F*). In accordance with this notion, we observed that ITK Tyr^{180} was required for maximal phosphorylation of ITK Tyr^{511}. Thus, our data strongly indicate that autophosphorylation of Tyr^{180} promotes phosphorylation of Tyr^{511}. In addition, the inhibition of reassociation of ITK $pTyr^{180}$ to TSAD upon activation of ITK by LCK, have the added advantage of leaving the ITK-SH3 domain free to recruit other targets to the activated kinase.

We have recently found that once activated by LCK, ITK will phosphorylate LCK Tyr^{192} in the LCK-SH2 domain, which increases the binding of LCK to some of its ligands, including TSAD and ITK (8). Importantly, LCK-SH2 domain mutated to mimic $Tyr(P)^{192}$ (*i.e.* Y192E) displays increased binding affinity to phosphopeptides representing ITK-$pTyr^{180}$ and ITK-$pTyr^{511}$ (8). It has been reported that one potential ligand for the ITK-SH2 domain is indeed the LCK-$pTyr^{192}$ (34). It is therefore possible that once the interaction between ITK and LCK has been promoted via their mutual interaction with TSAD through their SH3 domains, TSAD, ITK and LCK are dynamically altering their interaction modes depending on the phosphorylation status of the three interacting partners.

At the start of the current study, the solution structure of the human ITK-SH3 domain was yet to be determined. We thus determined the ITK-SH3 domain solution structure using NMR spectroscopy, and found that it is similar to the structure of the mouse ITK-SH3 domain (25). SH3 domains typically interact with peptides adopting a polyproline II helix, and the canonical PxxP motif commonly found in SH3 ligands ensures the formation of such a regular helix, with exactly three aa per turn (35). The flat binding surface of SH3 domains with two hydrophobic grooves lined mainly by aromatic residues is ideally suited to accommodate the xP dipeptides that form the base of the polyproline helix (x most often being a hydrophobic amino acid). However, some SH3 domains also bind to non-classical motifs, like the GRB2 SH3 binding to xxxRxxKP (36), the SKAP55 SH3 domain binding to RKxxYxxY (37), the PEX5P SH3 domain binding to WxxxFxxLE (38), the EPS8 SH3 domain binding to PxxDY (39) and the GADS C-terminal SH3 domain binding to the RxxK motif of SLP-76 (40,41).

Our initial NMR work involved the C-terminal ITK binding TSAD peptide aa262–269 I**P**VPRHRP based on the results obtained upon mutagenesis of Pro^{263}. TSAD aa262–269 lacks a PxxP motif and so the interaction of ITK SH3 with TSAD at this site can be added to the list of non-conventional SH3 binding motifs. Moreover, in contrast to the classic type I or II ligands of SH3 domains, where a terminal basic residue determines the binding orientation of the peptide on the SH3 binding surface (15), our data suggest that in this TSAD peptide, the hydrophobic aa Ile^{262} occupies this anchoring position. Thus, although the TSAD aa262–-269 peptide binding to ITK SH3 is a partial class II ligand with positively charged aa in the C terminus, our data suggests that its binding orientation on ITK SH3 is similar to that of class I ligands.

In conclusion, we have used biochemical analyses as well as NMR spectroscopy to analyze ITK SH3 and LCK SH3 interactions with TSAD. Our data indicate that LCK and ITK binding to TSAD is complex and may be characterized by simultaneously binding of the ITK- and LCK-SH3 domains to the TSAD PRR under some conditions and sequential binding of the ITK- and LCK-SH3 domains under other conditions. Further molecular mapping of the interaction between TSAD, ITK and LCK is required to understand the temporal dynamics of this tri-

molecular complex. In particular it will be important to characterize formation of this protein complex using larger fragments or full-length proteins since multi-valency may play a significant role in organizing the architecture of the functional TSAD based signaling complex.

Experimental procedures

Cells

Human embryonal kidney 293T cells were cultured in RPMI-1640 supplemented with L-glutamine, 5–10% fetal calf serum (FCS), 1 mM sodium pyruvate, 1 mM non-essential amino acids and 100 units/mL penicillin and 100 µg/mL streptomycin (all from GIBCOBRL®, ThermoFisher Scientific).

Plasmids

The pGex-2T with insert encoding intact or mutated tryptophan to lysine at position 208 (W208K) murine ITK-SH3–domain glutathione-*S*-transferase (GST) fusion protein (aa171–230 of ITK) and the pGex-6P-1 construct encoding human LCK SH3 were previously described (17,18,42). The pEF-Myc-ITK was kindly provided by Professor Leslie Berg. The pEF-LCK was kindly provided by Dr. Tomas Mustelin. LCK SH3 with a C-terminal hemagglutinin tag (HA) was constructed by amplifying the LCK SH3 sequence with a C-terminal primer encoding for this epitope, and the PCR product was cloned into the pGex-6P1 vector. The resulting construct yields a GST-tagged and HA-tagged LCK-SH3 domain. The human ITK-SH3 domain (aa168–232) was isolated from a human cDNA library (4) using PCR and sub cloned into pGex-6P-1 to generate the GST fusion protein expression construct. TSAD cDNA encoding TSAD wild type sequence or TSAD containing a deletion of aa239–274, aa239–256 or aa257–274 cloned into the expression vector pEF-HA (17) were used for transient expression of HA-tagged TSAD in eukaryote cells. Mutations of TSAD P247A and P263A in the pEF-HA-TSAD expression vectors, of ITK-Y180F and ITK-Y180E in ITK SH3 in the pGex-6P-1 vector as well as the pEF-Myc-ITK vector and of W208K in the pEF-Myc-ITK vector were performed using QuickChange mutagenesis and appropriate custom made primers. The sequences of all constructs were verified by sequencing.

Protein preparation

GST-SH3 domains were expressed in *E. coli* BL21(DE3). Cells were grown at 25 °C, until optical density (measured at 600 nm) reached 0.6. Isopropyl β-D-thiogalactopyranoside (IPTG) was then added to a final concentration of 0.2 mM to induce protein expression. In LB medium, the culture was incubated with IPTG for five hours, while in minimal medium (6 g/L glucose, 5 g/L Na_2PO_4, 3 g/L KH_2PO_4, 1 g/L $^{15}NH_4Cl$, 0,5 g/L NaCl, 0.12 g/L $MgSO_4$, 10 mg/L $CaCl_2$) incubation with IPTG was carried out overnight (~15 hours) at 15 °C. Minimal medium was used when incorporation of ^{15}N and ^{13}C was needed. The bacteria were then pelleted and resuspended in phosphate buffer (75 mM KH_2PO_4, 50 mM NaCl, 0,1 mM DTT, pH 7.4) containing lysozyme (1 mM) and frozen at -80 °C. After thawing, PMSF (1 mM) and DNase (5 µg/ml) were added, and the lysate was gently mixed at 4 °C for 8-16 hours. Upon completed lysis, the debris was removed by centrifugation (20 000 g, 4 °C, 15 min). Fusion protein was purified by Glutathione Sepharose™ 4B beads (Amersham Biosciences) in a batch mode as described by the manufacturer. Briefly, lysate and Glutathione Sepharose™ 4B beads were mixed and incubated with gentle agitation at 4 °C overnight. Beads were subsequently washed extensively in phosphate buffer (75mM KH_2PO_4, 50 mM NaCl, 0,1 mM DTT, pH7.4) prior to cleavage of the GST fusion protein with the appropriate protease (thrombin (Amersham Biosciences) or PreScission™ Protease (Amersham Biosciences). The purity and integrity of the purified proteins was analyzed by SDS-PAGE followed by Coomassie Brilliant Blue (BioRad) staining. Protein concentration was measured by NanoDrop spectrophotometry (Thermo Scientific, Wilmington, DE) at a wave length of 280 nm and a theoretically obtained extinction coefficient (ProtParam). Purity of NMR-samples typically exceeded 90%. If necessary, further concentration of the protein samples was performed using Amicon Ultra-15 centrifugal filter units (Millipore). NMR-samples were supplemented with 2,2-dimethyl-2-silapentane-5-sulfonate sodium salt (DSS) (Larodan Fine Chemicals AB, Malmö, Sweden) to a final concentration of 0.2 mM for internal chemical

shift referencing. 5% of D_2O was added to the samples to provide lock signal. Structure determination was performed for protein dissolved in 20 mM phosphate buffer, pH 6.5.

Peptides

Peptides derived from the human TSAD PRR aa248–268 (*LLRPKPPIPAKPQLPPEVYTIPVPRHR#), aa242–258 (*LLRPKPPIPAKPQLPPE#), aa254–268 (*QLPPEVYTIPVPRHR#), aa262–269 (*IPVPRHRP#), aa262–278 (*IPVPRHRPAPRPKPSNP#) and aa271–278 (*PRPKPSNP #) were synthesized with blocked ends (* and #) by GeneScript or Pepscan Systems to more than 99% purity as estimated by HPLC. The IPVPRHRP peptide was also custom synthesized with an N-terminal 2,2,6,6-tetramethyl-piperidine-1-oxyl-4-amino-4-carboxyl-acid (TOAC) label by Anaspec (San Jose, CA).

Peptide array

Peptide arrays were synthesized on nitrocellulose membranes using a MultiPep automated peptide synthesizer (INTAVIS Bioanalytical Instruments AG, Germany) as described (43,44). Peptide array membranes were probed with GST-tagged SH3 domains (100 μg/ml) and blotted with mouse anti-GST antibody (Santa Cruz Biotechnology, Santa Cruz, CA) and anti-mouse HRP secondary antibody followed by chemiluminescent detection.

Transfection of cells

Transient transfections of 293T cells took place for 5–6 hours with 1–2 μg DNA in 25 μl lipofectin (GIBCO-BRL) or 16,125 μg of polyethyleneimine (Polysciences Inc, Warrington, PA). Transfected cells were further propagated for 16–24 hours in the presence of FCS (5 % final concentration).

Cell lysis and pull-down experiments

293T cells were transfected with different HA-tagged constructs of TSAD cDNA. Cells were lysed in buffer containing 1% Igepal CA-630 (Sigma), 25 mM Tris (pH7.5), 100 mM NaCl, 20 mM NaF, 1 mM $NaVO_3$ and 10 μg/ml of antipain, chymostatin, leupeptin and pepstatin A (Sigma-Aldrich). Lysates representing $2{\cdot}10^6$–$4{\cdot}10^6$ transfected cells were pre-cleared three times for 30 min-1 hour with a 2:1 GST-Glutathione 4B Sepharose™ beads : 4B Sepharose™ beads mixture at 4 °C. Pre-cleared lysates were added to aliquots of GST-ITK-SH3 or GST-LCK-SH3 bound to Glutathione 4B Sepharose™ beads and gently mixed at 4 °C for 1 hour. Finally the beads were washed three times using lysis buffer and boiled in SDS loading buffer containing mercaptoethanol, before separation of proteins on SDS-PAGE. *In vitro* pull-down experiments using isolated HA-tagged LCK-SH3 domains and GST-tagged ITK-SH3 domains bound to Glutathione 4B SepharoseTM beads SH3 domains were performed in buffer containing 1% Igepal CA-630, 25 mM Tris (pH7.5), 100 mM NaCl, 2% BSA and 10 μM of each SH3 domain and the indicated amount of TSAD peptides. Prior to use in the in vitro pull-down assay, the GST-ITK-SH3 Glutathione 4B SepharoseTM beads were mixed 1:2 (bead volume) with GST Glutathione 4B SepharoseTM beads.

Immunoprecipitation experiments — 293 T cells were transfected with HA-tagged TSAD constructs along with LCK and myc tagged ITK WT or ITK W208K. The cells were lysed in buffer containing 0.1% LDS, 0,5-1% Triton X-100, 50mM HEPES, 0.05 M lithium chloride, 0.5 mM PMSF, 2.5 mM EDTA (pH 8.0), 1 mM $NaVO_3$,10 μg/ml of antipain, chymostatin, leupeptin and pepstatin A (Sigma-Aldrich) and 1 mg/ml DNAse for 45 min. The lysate was sonicated briefly to fragment the DNA. The lysate was preabsorbed twice at 4 °C for 30 min using Dynabeads® Protein G (Life Technologies). The preabsorbed lysate was added to the Dynabeads® Protein G coated with anti-Myc-antibody (clone 9E10, Sigma) or anti-TSAD antibody (4) for 1 hour in rotating wheel at 4°. The beads were washed three times using lysis buffer and boiled in loading buffer containing 2-mercaptoethanol before separation of proteins on SDS-PAGE. Proteins were detected by using the following primary antibodies: anti-ITK antibody (Médimabs, clone 2F12), anti-LCK (Santa Cruz, clone 3A5), anti-HA1.1 (Bio Site, clone 16B12), anti pY (clone 4G10) or anti-pY511 ITK (clone

24a/Btk, BD Biosciences) in Tris buffered saline (TBS, pH 7.4) with 0.1 % Tween (Sigma Aldrich)/ 3% bovine serum albumin (BSA) (Biotest) or 3 % skimmed milk (Sigma Aldrich), Signals were detected by horse radish peroxidase (HRP)-conjugated goat anti-mouse IgG or goat anti-rabbit IgG (Jackson ImmunoResearch Laboratories) and Super Signal® west Pico Stable Peroxide Solution (Pierce) (5). Images of scanned WB films were analyzed using ImageJ software (45).

NMR spectroscopy

The following NMR experiments were performed to assign the backbone chemical shifts and determine structural restraints: ^{15}N-HSQC, ^{13}C-HSQC, ^{15}N- NOESYHSQC, ^{13}C-NOESYHSQC, HNHA, HNCA, CBCACONH, CBCANH, HNCO, HNCACO, HNCOCA,(H)CCCONH, HCCCONH, HBHACONH, HBHANH HCCH-TOCSY (46). ^{1}H-^{15}N NOESY with a mixing time of 3s were performed to investigate the relaxation properties of the protein (47). Experiments for structure determination were run on a 600 MHz Bruker Avance II spectrometer with four channels and a 5 mm TCI cryo-probe at 25ºC. 1H-15N-HSQC titration experiments were recorded at 25 °C on Varian INOVA spectrometers at 600 MHz or Bruker Avance II spectrometer at 600 MHz or 700 MHz. All instruments were equipped with a cryo-probes..

Data Processing

Data were processed using Topspin 2.1 (Bruker Biospin). DSS was used as a chemical shift standard, and ^{13}C and ^{15}N data were referenced using frequency ratios as described by Wishart et al. (48). Time-domain to frequency-domain processing was carried out using NMRPipe (49) or TopSpin software respectively, and subsequent analysis of titration experiments was performed using Sparky.

Assignment

For visualization and assignment the computer program CARA (50) was used. The spectra were assigned using standard methods (46). The chemical shifts are deposited in the Biological Magnetic Resonance Data Bank (BMRB) with the access code 18119.

Structure calculation and docking of TSAD-peptide to the ITK SH3 structure

The ^{15}N and ^{13}C-NOESY-HSQC spectra were peak picked using CARA (50). NOESY upper distance constraints were generated by the CANDID routine in CYANA 3.0 (51). Torsion angle constraints were determined from the chemical shifts by the application of TALOS (52). Temperature dependence more positive than -4.5ppb/K for the amide proton was taken as a proof of an existence of a hydrogen bond (53). Hydrogen bond and torsion angle restraints were introduced in the final stage of structure determination. 100 structures were calculated using CYANA 3.0 and the 20 structures with the lowest energy were kept in the structure ensemble.[2]

NMR titration

The NMR samples consisted of a uniformly ^{15}N-labelled recombinant ITK-SH3 or LCK-SH3 protein of human origin dissolved in phosphate buffer (75 mM KH_2PO_4, 50 mM NaCl, 0.1 mM DTT, pH 7.4) at concentrations ranging from 40 μM–300 μM, containing 5% D_2O. Titration was done by stepwise addition of a defined amount of TSAD peptide or unlabeled SH3 domain, dissolved in the same phosphate buffer, to the LCK-SH3 and/or ITK-SH3 NMR-samples. At each step, a ^{15}N-HSQC spectrum was recorded. ^{1}H and ^{15}N chemical shifts were referenced to DSS. The chemical shift deviations were quantified using the formula: $\Delta_{av} = [(\Delta_{HN})^2 + (0.2\Delta_N)^2]^{1/2}$ (54), where Δ_{HN} and Δ_N correspond to the amide proton and nitrogen chemical shift changes upon peptide binding respectively. The dissociation constants were derived from binding curves generated using the Matlab (version 5.3.1, The Mathworks Inc.) suite of programs by plotting Δ_{ave} versus ligand concentration.

TOAC experiment

A ^{15}N-HSQC NMR spectrum of uniformly ^{15}N-labelled, recombinant, ITK SH3 dissolved in phosphate buffer (as described above) at a concentration of approximately 500 μM was recorded after adding N-terminally TOAC- labeled peptide: TOAC-IPVPRHRP to a

final concentration of 1mM. In addition, a ^{15}N-HSQC NMR spectrum of the same solution, adjusted to 400 μM Na-ascorbate, was recorded. Addition of the reducing agent Na-ascorbate abolishes the effect the TOAC label has on the spectrum.

Docking model of IPVPRHRP to ITK SH3

The peptide structure of IPVPRHRP was generated by mutating the polypeptide of 1VZJ using pymol. Docking of the peptide to ITK SH3 was performed using the HADDOCK server (26). Ambiguous restraints where defined between residues Thr^{184}, Asp^{186}, Glu^{189}, Leu^{192}, His^{207}, Trp^{208}, Trp^{209}, Val^{211}, Tyr^{220}, Val^{221}, Ser^{223} and Tyr^{225} and the peptide IPVPRHRP.

Acknowledgments: Leslie Berg and Tomas Mustelin are thanked for providing valuable reagents. The technical assistance of Bjørg Simonsen and Lise Koll is highly appreciated.

Competing interests: The authors declare no financial conflict of interest that might be construed to influence the results or interpretation of this manuscript.

References

1. Koretzky, G. A., and Myung, P. S. (2001) Positive and negative regulation of T-cell activation by adaptor proteins. *Nat.Rev.Immunol.* **1**, 95-107
2. Mustelin, T., and Tasken, K. (2003) Positive and negative regulation of T-cell activation through kinases and phosphatases. *Biochem.J.* **371**, 15-27
3. Felices, M., Falk, M., Kosaka, Y., and Berg, L. J. (2007) Tec kinases in T cell and mast cell signaling. *Adv.Immunol.* **93**, 145-184
4. Spurkland, A., Brinchmann, J. E., Markussen, G., Pedeutour, F., Munthe, E., Lea, T., Vartdal, F., and Aasheim, H. C. (1998) Molecular cloning of a T cell-specific adapter protein (TSAD) containing an Src homology (SH) 2 domain and putative SH3 and phosphotyrosine binding sites. *J Biol Chem* **273**, 4539-4546
5. Granum, S., Sundvold-Gjerstad, V., Dai, K. Z., Kolltveit, K. M., Hildebrand, K., Huitfeldt, H. S., Lea, T., and Spurkland, A. (2006) Structure function analysis of *SH2D2A* isoforms expressed in T cells reveals a crucial role for the proline rich region encoded by *SH2D2A* exon 7. *BMC.Immunol.* **7**, 15
6. Choi, Y. B., Kim, C. K., and Yun, Y. (1999) Lad, an adapter protein interacting with the SH2 domain of p56lck, is required for T cell activation. *J Immunol* **163**, 5242-5249
7. Rajagopal, K., Sommers, C. L., Decker, D. C., Mitchell, E. O., Korthauer, U., Sperling, A. I., Kozak, C. A., Love, P. E., and Bluestone, J. A. (1999) RIBP, a novel Rlk/Txk- and itk-binding adaptor protein that regulates T cell activation. *J.Exp.Med.* **190**, 1657-1668
8. Granum, S., Sundvold-Gjerstad, V., Gopalakrishnan, R. P., Abrahamsen, G., Berge, T., Koll, L., Sørlie, M., and Spurkland, A. (2014) Itk and the adapter TSAD co-operate to promote phosphorylation dependent altered specificity of Lck. *Science Signaling* **7**, p. ra118
9. Sundvold, V., Torgersen, K. M., Post, N. H., Marti, F., King, P. D., Rottingen, J. A., Spurkland, A., and Lea, T. (2000) T cell-specific adapter protein inhibits T cell activation by modulating Lck activity. *J.Immunol.* **165**, 2927-2931
10. Berge, T., Sundvold-Gjerstad, V., Granum, S., Andersen, T. C., Holthe, G. B., Claesson-Welsh, L., Andreotti, A. H., Inngjerdingen, M., and Spurkland, A. (2010) T cell specific adapter protein (TSAD) interacts with Tec kinase ITK to promote CXCL12 induced migration of human and murine T cells. *PLoS.ONE.* **5**, e9761
11. Drappa, J., Kamen, L. A., Chan, E., Georgiev, M., Ashany, D., Marti, F., and King, P. D. (2003) Impaired T cell death and lupus-like autoimmunity in T cell-specific adapter protein-deficient mice. *J.Exp.Med.* **198**, 809-821
12. Smith, C. I., Islam, T. C., Mattsson, P. T., Mohamed, A. J., Nore, B. F., and Vihinen, M. (2001) The Tec family of cytoplasmic tyrosine kinases: mammalian Btk, Bmx, Itk, Tec, Txk and homologs in other species. *Bioessays* **23**, 436-446
13. Kuriyan, J., and Cowburn, D. (1997) Modular peptide recognition domains in eukaryotic signaling. *Annu.Rev.Biophys.Biomol.Struct.* **26**, 259-288
14. Tran, T., Hoffmann, S., Wiesehan, K., Jonas, E., Luge, C., Aladag, A., and Willbold, D. (2005) Insights into human Lck SH3 domain binding specificity: different binding modes of artificial and native ligands. *Biochemistry* **44**, 15042-15052

15. Feng, S., Chen, J. K., Yu, H., Simon, J. A., and Schreiber, S. L. (1994) Two binding orientations for peptides to the Src SH3 domain: development of a general model for SH3-ligand interactions. *Science* **266**, 1241-1247
16. Granum, S., Andersen, T. C., Sorlie, M., Jorgensen, M., Koll, L., Berge, T., Lea, T., Fleckenstein, B., Spurkland, A., and Sundvold-Gjerstad, V. (2008) Modulation of Lck Function through Multisite Docking to T Cell-specific Adapter Protein. *J.Biol.Chem.* **283**, 21909-21919
17. Sundvold-Gjerstad, V., Granum, S., Mustelin, T., Andersen, T. C., Berge, T., Shapiro, M. J., Shapiro, V. S., Spurkland, A., and Lea, T. (2005) The C terminus of T cell-specific adapter protein (TSAD) is necessary for TSAD-mediated inhibition of Lck activity. *Eur J Immunol* **35**, 1612-1620
18. Bunnell, S. C., Henry, P. A., Kolluri, R., Kirchhausen, T., Rickles, R. J., and Berg, L. J. (1996) Identification of Itk/Tsk Src homology 3 domain ligands. *J.Biol.Chem.* **271**, 25646-25656
19. Wilcox, H. M., and Berg, L. J. (2003) Itk phosphorylation sites are required for functional activity in primary T cells. *J.Biol.Chem.* **278**, 37112-37121
20. Joseph, R. E., Fulton, D. B., and Andreotti, A. H. (2007) Mechanism and functional significance of Itk autophosphorylation. *J.Mol.Biol.* **373**, 1281-1292
21. Obenauer, J. C., Cantley, L. C., and Yaffe, M. B. (2003) Scansite 2.0: Proteome-wide prediction of cell signaling interactions using short sequence motifs. *Nucleic Acids Res.* **31**, 3635-3641
22. Cory, G. O., MacCarthy-Morrogh, L., Banin, S., Gout, I., Brickell, P. M., Levinsky, R. J., Kinnon, C., and Lovering, R. C. (1996) Evidence that the Wiskott-Aldrich syndrome protein may be involved in lymphoid cell signaling pathways. *Journal of Immunology* **157**, 3791-3795
23. Bunnell, S. C., Diehn, M., Yaffe, M. B., Findell, P. R., Cantley, L. C., and Berg, L. J. (2000) Biochemical interactions integrating Itk with the T cell receptor-initiated signaling cascade. *J.Biol.Chem.* **275**, 2219-2230
24. Cavanagh, J., Fairbrother, W. J., Palmer III, A. G., Rance, M., and Skelton, N. J. (2007) *Principles and Practice of Protein NMR Spectroscopy*, 2nd ed., Elsevier Acacemic Press, Burlington, MA, USA
25. Severin, A., Fulton, D. B., and Andreotti, A. H. (2008) Murine Itk SH3 domain. *J Biomol.NMR* **40**, 285-290
26. de Vries, S. J., van, D. M., and Bonvin, A. M. (2010) The HADDOCK web server for data-driven biomolecular docking. *Nat.Protoc.* **5**, 883-897
27. Pear, W. S., Nolan, G. P., Scott, M. L., and Baltimore, D. (1993) Production of high-titer helper-free retroviruses by transient transfection. *Proc Natl Acad Sci U S A* **90**, 8392-8396
28. Kagan, J. C., Magupalli, V. G., and Wu, H. (2014) SMOCs: supramolecular organizing centres that control innate immunity. *Nat.Rev.Immunol*
29. Li, P., Banjade, S., Cheng, H. C., Kim, S., Chen, B., Guo, L., Llaguno, M., Hollingsworth, J. V., King, D. S., Banani, S. F., Russo, P. S., Jiang, Q. X., Nixon, B. T., and Rosen, M. K. (2012) Phase transitions in the assembly of multivalent signalling proteins. *Nature* **483**, 336-340
30. Houtman, J. C., Yamaguchi, H., Barda-Saad, M., Braiman, A., Bowden, B., Appella, E., Schuck, P., and Samelson, L. E. (2006) Oligomerization of signaling complexes

by the multipoint binding of GRB2 to both LAT and SOS1. *Nat.Struct.Mol.Biol.* **13**, 798-805

31. Kortum, R. L., Balagopalan, L., Alexander, C. P., Garcia, J., Pinski, J. M., Merrill, R. K., Nguyen, P. H., Li, W., Agarwal, I., Akpan, I. O., Sommers, C. L., and Samelson, L. E. (2013) The ability of Sos1 to oligomerize the adaptor protein LAT is separable from its guanine nucleotide exchange activity in vivo. *Sci.Signal.* **6**, ra99
32. Phillip, Y., and Schreiber, G. (2013) Formation of protein complexes in crowded environments--from in vitro to in vivo. *FEBS letters* **587**, 1046-1052
33. Boeynaems, S., Alberti, S., Fawzi, N. L., Mittag, T., Polymenidou, M., Rousseau, F., Schymkowitz, J., Shorter, J., Wolozin, B., Van Den Bosch, L., Tompa, P., and Fuxreiter, M. (2018) Protein Phase Separation: A New Phase in Cell Biology. *Trends in cell biology* **28**, 420-435
34. Koytiger, G., Kaushansky, A., Gordus, A., Rush, J., Sorger, P. K., and MacBeath, G. (2013) Phosphotyrosine signaling proteins that drive oncogenesis tend to be highly interconnected. *Mol.Cell Proteomics.* **12**, 1204-1213
35. Li, S. S. (2005) Specificity and versatility of SH3 and other proline-recognition domains: structural basis and implications for cellular signal transduction. *Biochem.J.* **390**, 641-653
36. Lewitzky, M., Kardinal, C., Gehring, N. H., Schmidt, E. K., Konkol, B., Eulitz, M., Birchmeier, W., Schaeper, U., and Feller, S. M. (2001) The C-terminal SH3 domain of the adapter protein Grb2 binds with high affinity to sequences in Gab1 and SLP-76 which lack the SH3-typical P-x-x-P core motif. *Oncogene* **20**, 1052-1062
37. Kang, H., Freund, C., Duke-Cohan, J. S., Musacchio, A., Wagner, G., and Rudd, C. E. (2000) SH3 domain recognition of a proline-independent tyrosine-based RKxxYxxY motif in immune cell adaptor SKAP55. *EMBO J.* **19**, 2889-2899
38. Barnett, P., Bottger, G., Klein, A. T., Tabak, H. F., and Distel, B. (2000) The peroxisomal membrane protein Pex13p shows a novel mode of SH3 interaction. *EMBO J.* **19**, 6382-6391
39. Mongiovi, A. M., Romano, P. R., Panni, S., Mendoza, M., Wong, W. T., Musacchio, A., Cesareni, G., and Di Fiore, P. P. (1999) A novel peptide-SH3 interaction. *EMBO J.* **18**, 5300-5309
40. Berry, D. M., Nash, P., Liu, S. K., Pawson, T., and McGlade, C. J. (2002) A high-affinity Arg-X-X-Lys SH3 binding motif confers specificity for the interaction between Gads and SLP-76 in T cell signaling. *Curr.Biol.* **12**, 1336-1341
41. Liu, Q., Berry, D., Nash, P., Pawson, T., McGlade, C. J., and Li, S. S. (2003) Structural basis for specific binding of the Gads SH3 domain to an RxxK motif-containing SLP-76 peptide: a novel mode of peptide recognition. *Mol.Cell* **11**, 471-481
42. Andreotti, A. H., Bunnell, S. C., Feng, S., Berg, L. J., and Schreiber, S. L. (1997) Regulatory intramolecular association in a tyrosine kinase of the Tec family. *Nature* **385**, 93-97
43. Kramer, A., and Schneider-Mergener, J. (1998) Synthesis and screening of peptide libraries on continuous cellulose membrane supports. *Methods Mol.Biol.* **87**, 25-39
44. Frank, R. (2002) High-density synthetic peptide microarrays: emerging tools for functional genomics and proteomics. *Comb.Chem.High Throughput.Screen.* **5**, 429-440

45. Schneider, C. A., Rasband, W. S., and Eliceiri, K. W. (2012) NIH Image to ImageJ: 25 years of image analysis. *Nat.Methods* **9**, 671-675
46. Sattler, M., Schleucher, J., and Griesinger, C. (1999) Heteronuclear multidimensional NMR experiments for the structure determination of proteins in solution employing pulsed field gradients. *Prog.Nucl.Magn.Reson.Spectr.*, 93-158
47. Renner, C., Schleicher, M., Moroder, L., and Holak, T. A. (2002) Practical aspects of the 2D 15N-[1h]-NOE experiment. *J.Biomol.NMR* **23**, 23-33
48. Wishart, D. S., Bigam, C. G., Yao, J., Abildgaard, F., Dyson, H. J., Oldfield, E., Markley, J. L., and Sykes, B. D. (1995) 1H, 13C and 15N chemical shift referencing in biomolecular NMR. *J.Biomol.NMR* **6**, 135-140
49. Delaglio, F., Grzesiek, S., Vuister, G. W., Zhu, G., Pfeifer, J., and Bax, A. (1995) NMRPipe: a multidimensional spectral processing system based on UNIX pipes. *J.Biomol.NMR* **6**, 277-293
50. Keller, R. L. J. (2004) *Optimizing the process of nuclear magnetic resonance spectrum analysis and computer aided resonance assignment. Thèse de doctorat.* Thèse de doctorat, ETH Zurich Thesis No. 15947, Switzerland
51. Herrmann, T., Guntert, P., and Wuthrich, K. (2002) Protein NMR structure determination with automated NOE assignment using the new software CANDID and the torsion angle dynamics algorithm DYANA. *J.Mol.Biol.* **319**, 209-227
52. Cornilescu, G., Delaglio, F., and Bax, A. (1999) Protein backbone angle restraints from searching a database for chemical shift and sequence homology. *J.Biomol.NMR* **13**, 289-302
53. Baxter, N. J., and Williamson, M. P. (1997) Temperature dependence of 1H chemical shifts in proteins. *J.Biomol.NMR* **9**, 359-369
54. Radhakrishnan, I., Perez-Alvarado, G. C., Parker, D., Dyson, H. J., Montminy, M. R., and Wright, P. E. (1999) Structural analyses of CREB-CBP transcriptional activator-coactivator complexes by NMR spectroscopy: implications for mapping the boundaries of structural domains. *J Mol.Biol.* **287**, 859-865
55. Marengere, L. E., Okkenhaug, K., Clavreul, A., Couez, D., Gibson, S., Mills, G. B., Mak, T. W., and Rottapel, R. (1997) The SH3 domain of Itk/Emt binds to proline-rich sequences in the cytoplasmic domain of the T cell costimulatory receptor CD28. *J.Immunol.* **159**, 3220-3229
56. Perez-Villar, J. J., O'Day, K., Hewgill, D. H., Nadler, S. G., and Kanner, S. B. (2001) Nuclear localization of the tyrosine kinase Itk and interaction of its SH3 domain with karyopherin alpha (Rch1alpha). *Int.Immunol* **13**, 1265-1274
57. Hansson, H., Okoh, M. P., Smith, C. I., Vihinen, M., and Hard, T. (2001) Intermolecular interactions between the SH3 domain and the proline-rich TH region of Bruton's tyrosine kinase. *FEBS Lett.* **489**, 67-70

FOOTNOTES

This work was supported by grants from the University of Oslo, the Norwegian Research Council (grant no 196386 and 214202), the Norwegian Cancer Society (grant no 163359 and 163361), Novo Nordisk Fonden, Unifor, Anders Jahres fond til vitenskapens fremme and the University of Oslo. PHB was supported by the Southeastern Norway Regional Health Authorities Technology Platform for Structural Biology (grant 2015095). We acknowledge the Research Council of Norway for their investment in the 600 MHz NMR spectrometer at the University of Oslo.

[1] The abbreviations used are: aa, amino acid; ITK, Inducible Tec kinase; LCK, Lymphocyte specific kinase; HA, Hemagglutinin; PRR, Proline rich region; PTKs, protein tyrosine kinases; SH3, SRC homology 3; TCR, T cell receptor; 2D, two dimensional; 3D, three dimensional; TOAC, 2,2,6,6-tetramethyl-piperidine-1-oxyl-4-amino-4-carboxylic-acid; TSAD, T cell specific adapter protein.

[2] The final structure ensemble of human ITK SH3 is deposited in the Protein Data Bank (PDB) with access code 2LMJ.

Table 1: Verified and putative ITK SH3 motifs

Protein	Sequence motif	Reference
TSAD	QLPPEVYTI**PVP**RH**RP**A	This paper
SLP-76	DRPPSGKTPQQP**PVP**PQ**RP**MA	(23)
CBL-B (human)	DVFDSASDPV**P**L**P**PA**RP**PTR	(18)
CD28	NMTPRR**P**G**P**TR**K**HYQP	(55)
RCH1α	SNLCRNKN**PAP**PIDAV	(56)
ITK/BTK PRR	K**P**L**P**PTP	(57)
Consensus	Ψ**P**Ψ**P**XX[R/K]	

Table 2: Constraints and structural statistics of ITK-SH3 NMR structure

Constraints	
NOE constraints	1,267
Intraresidue	267
Sequential (ji – jj = 1)	337
Medium range (1 < ji – jj < 5)	139
Long range (ji – jj > 5)	524
Hydrogen bonds/constraints	17/34
Dihedral angle constraints	80
Total no. of constraints	1381
Structural statistics	
Constraint violations	
Distance constraints (Å)	0.0063 ± 0.0008
Dihedral angle constraints (°)	0.57 ± 0.04
Max. distance constraint violation (Å)	<0.01
Max. dihedral constraint violation (°)	<4
rms difference to mean structure residues 8 to 65	
Backbone (Å)	0.29± 0.09
Heavy atoms (Å)	0.98± 0.15
Ramachandran statistics	
% in core regions	84.1
% in allowed regions	15.9
% in generous regions	0
% in disallowed regions	0
CYANA Å	
Total	0.54± 0.0616

Table 3. Kd values (μM) estimated from HSQC titration experiments

	SH3 domain	
Peptide	ITK	LCK
TSAD aa242–256	150±12	69±3
TSAD aa242–268	123±22	161±75
TSAD aa254–268	n.d.	n.d.

n.d.: not determined

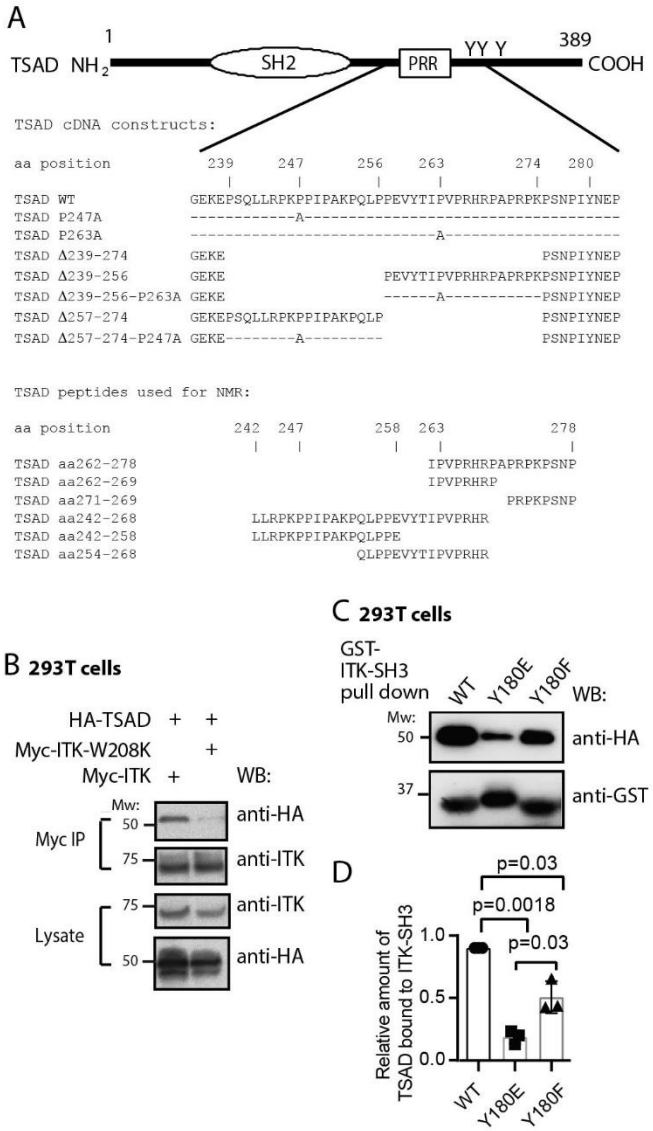

FIGURE 1. Non-phosphorylated ITK-SH3 domain is required for ITK binding to TSAD. *A*, Schematic drawing of TSAD including the SH2 domain, the proline rich region (PRR) and the three C-terminal tyrosines. The core sequences encoded by the TSAD cDNA constructs and the TSAD peptides used for transfection of cells and for NMR experiments respectively in this paper, are also indicated. *B*, Co-immunoprecipitation experiment showing dependence of ITK-TSAD interaction on SH3 domain of ITK. 293T cells were transfected with the indicated cDNA plasmids. Myc-tagged ITK proteins were immunoprecipitated from the cell lysates, followed by immunoblotting with the indicated antibodies. The result is one representative of two experiments. *C* and *D*, ITK-SH3 domains mutated for Tyr^{180} display reduced interaction with TSAD. *C.* Pull-down experiment using ITK-SH3 domains with the indicated mutations was performed using lysates of 293T cells transiently transfected with HA-tagged wild type and mutated TSAD cDNA. Pull-downed proteins were immunoblotted with the indicated antibodies. *D.* Graph represents relative amount of TSAD interacting with ITK SH3 in the experiment shown in *C*. Signals were quantified by ImageJ analysis (n=3, mean +- SD).

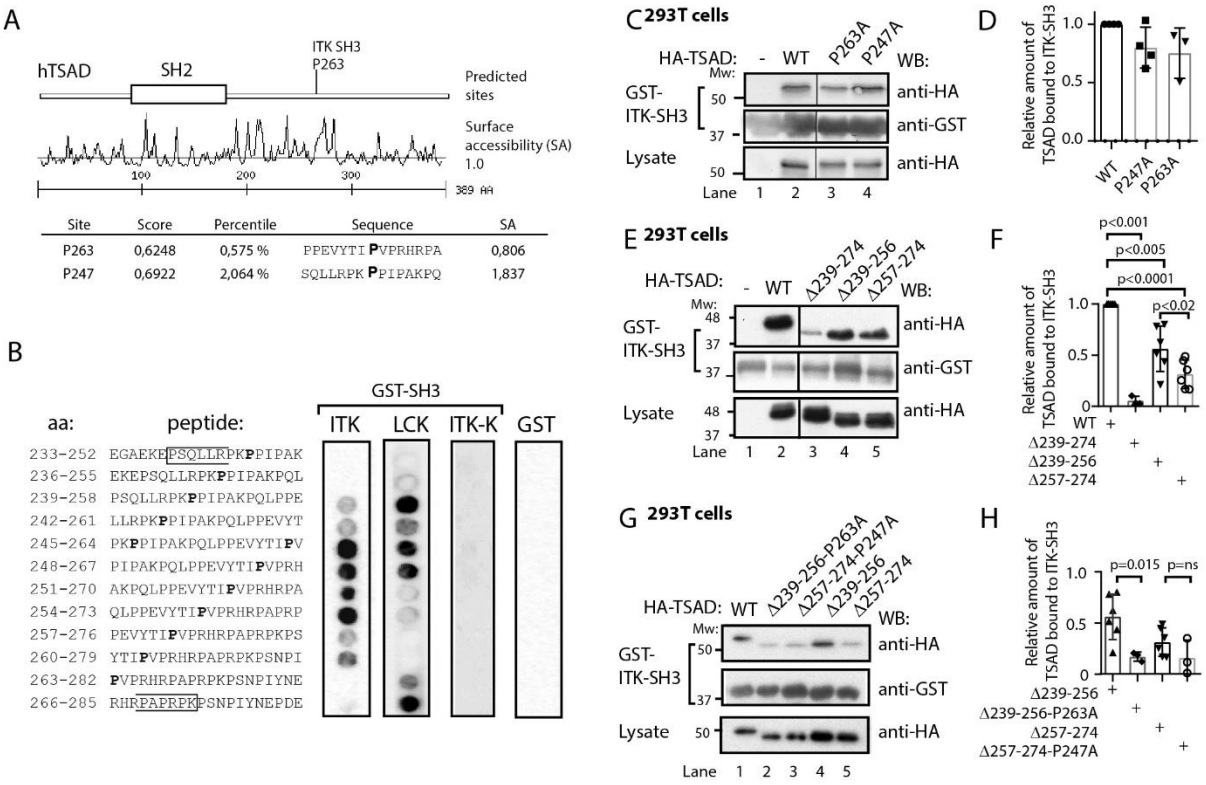

FIGURE 2. LCK SH3 and ITK SH3 bind to overlapping peptides in TSAD PRR. *A*, Scansite prediction of ITK-SH3 binding sites on TSAD. *B*, Peptide array mapping of LCK-SH3 and ITK-SH3 binding sites on TSAD. The amino acid sequence of the peptide in each of the spots is given to the left. Right panels show the results of probing the arrays with the indicated recombinant proteins GST-ITK SH3, GST-LCK SH3, GST-ITK SH3 mutated (W208K or ITK-K) or GST alone respectively. Results from 12 of the 14 tested peptides are shown. Pro^{247} and Pro^{263} are indicated in bold. The brackets defines the borders of TSAD aa239-274. *C* and *D*, Mutations of the predicted prolines to alanines fail to abolish binding of ITK SH3 to TSAD. Pull-down experiment was performed using GST-ITK SH3 and lysates of 293T cells transiently transfected with HA-tagged wild type and mutated TSAD cDNA. Pull-downed protein and lysate were immunoblotted with the indicated antibodies. *D*, Graph represents relative amount of TSAD interacting with ITK SH3 in the experiment shown in *C*. Signals were quantified by ImageJ analysis (n=3, mean +- SD). *E* and *F*, Deletion of either the Pro^{247} (aa239–256) or the Pro^{263} (aa257–274) region reduces binding of ITK SH3 to TSAD. Pull-down experiment performed as in *C*. *F*, Graph represents ImageJ analysis as in *D* of data shown in *E* (n=3 or 6, mean +- SD). *G* and *H*, Additional mutation of Pro^{263} further reduce binding of ITK SH3 to TSAD 257–274. Pull-down experiment performed as in *C*. *H*, Graph represents ImageJ analysis as in *D* of data shown in *G*. Relative amount of TSAD interacting with ITK SH3 WT in each experiment is set to 1 (not shown) (n=3, mean +- SD).

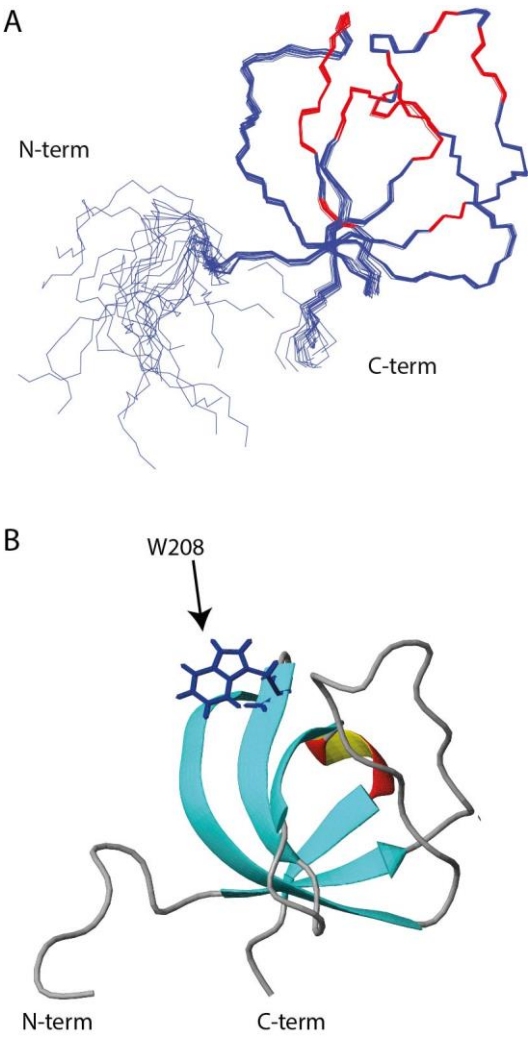

FIGURE 3. The human ITK-SH3 domain solution structure. *A*, The backbone trace of the 20 structures comprising the lowest energy NMR ensemble is shown. Red color indicates residues affected by ligand binding. *B*, Ribbon representation of one of the ITK-SH3 domain structures shown in *A*. The tryptophan at position 208, which is critical for polyproline ligand binding, is indicated.

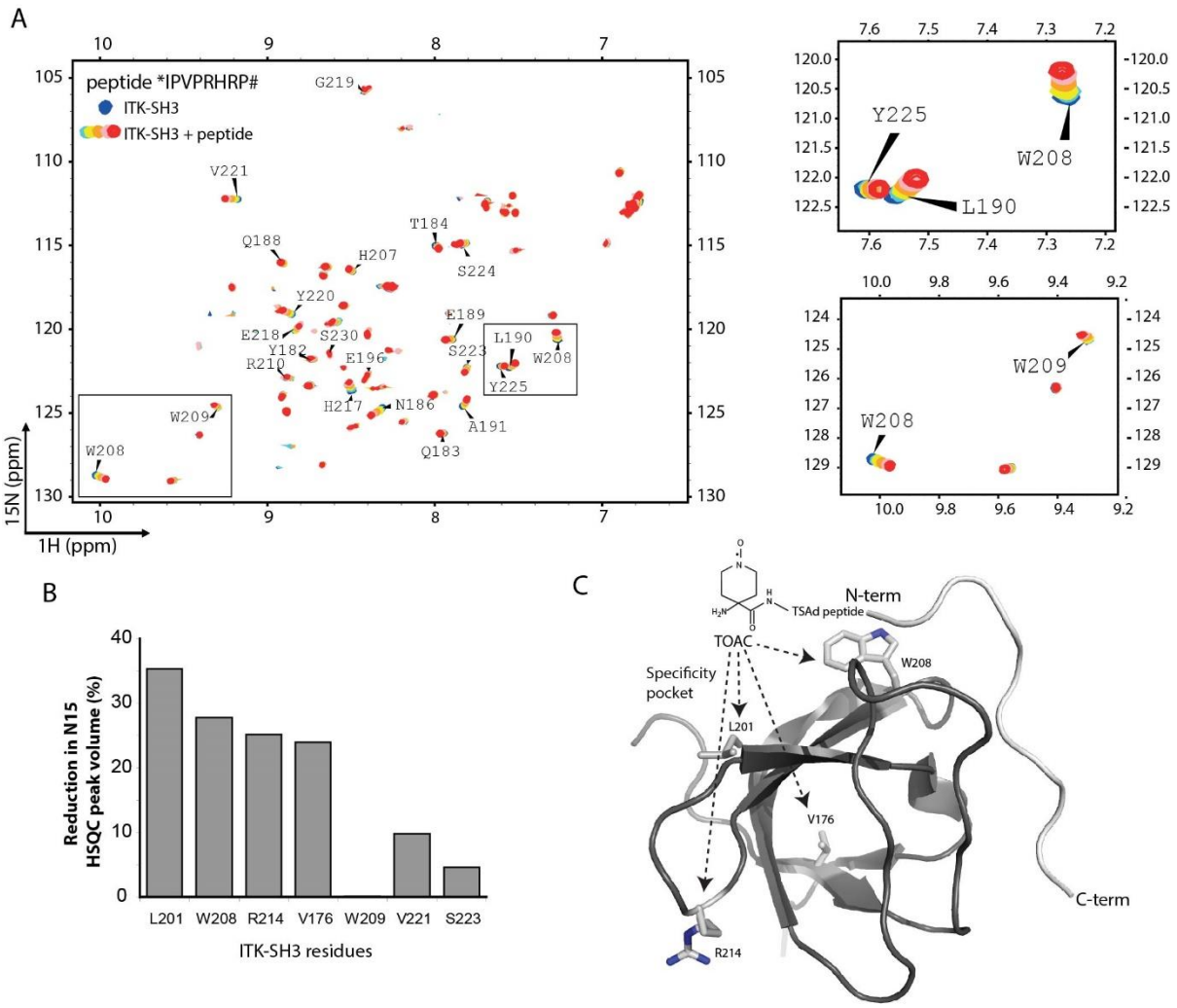

FIGURE 4. The human ITK-SH3 domain binds to TSAD aa262–269 in a class I orientation. *A*, 1H-15N HSQC of human 20 μM ITK-SH3 domain without (blue) and with increasing amounts (200 μM to 1 mM, light blue to green-red) of TSAD aa262–269 (*I**P**VPRHRP#) added. Chemical shifts changes are observed indicating binding of the peptide to the ITK-SH3 domain. *B*, TOAC experiment. HSQC experiments using TSAD aa262–269 with an N-terminal TOAC aa were performed with and without a reducing agent (ascorbate) added to the solution to remove the effect of the TOAC aa. TOAC aa causes broadening of peaks in the NMR spectrum representing neighboring aa. Graph shows the percent reduction in peak volume of the four most affected aa (Leu^{201}, Trp^{208}, Arg^{214} and Val^{176}) in addition to three aa (Trp^{209}, Val^{221} and Ser^{223}) that the titration experiments had identified to be affected by peptide binding. *C*, 3D structure of human ITK-SH3 domain with the TOAC-labeled TSAD peptide aa262–269 (light grey) docked onto the SH3 domain using constraints given by the aa most affected by the peptide titration. The amino- and carboxy-termini of the TSAD peptide are labeled N-term and C-term, respectively. The location of Leu^{201}, Trp^{208}, Arg^{214} and Val^{176} (resonances most affected by TOAC) are shown on the SH3 structure.

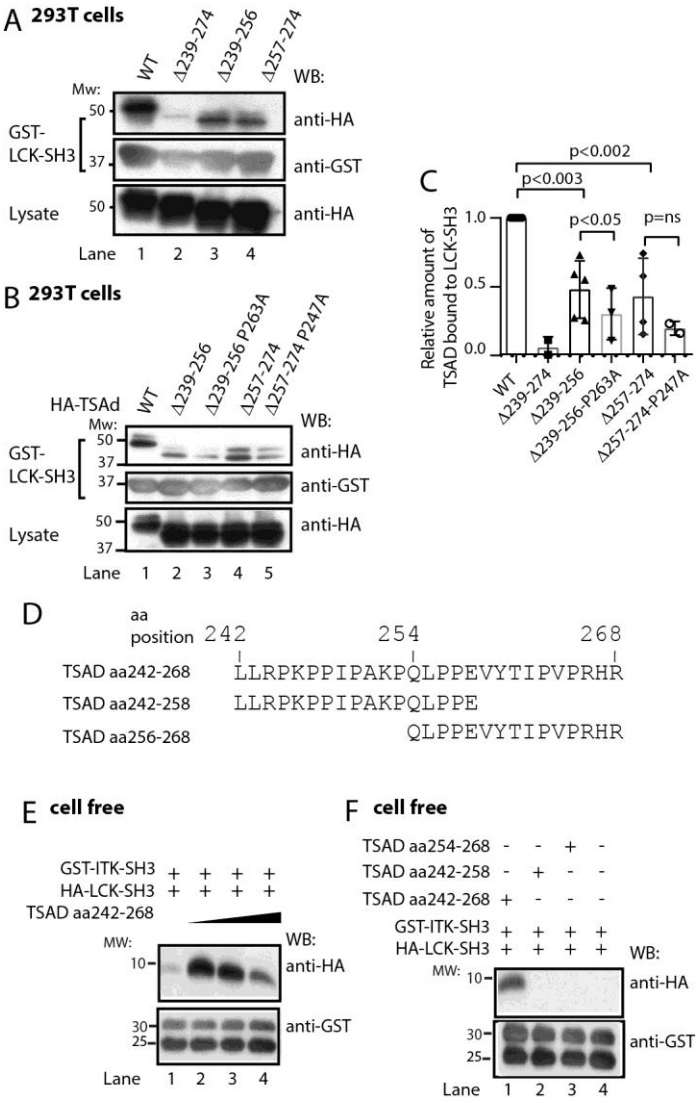

FIGURE 5. LCK SH3 and ITK SH3 may bind simultaneously to TSAD aa242–268. *A-C*, LCK SH3 interacts with both TSAD aa239–256 and aa257–274. Additional mutation of Pro^{247} or Pro^{263} further reduces binding. *A* and *B*, Pull-down experiment in 293T cells using the same TSAD constructs as in Fig. 2*E* and Fig. 2*G* respectively. Pull-downed proteins and lysates are probed with the indicated antibodies. *C*, Graph represents ImageJ analysis of data shown in *A* and *B* (n=3, mean +-SD). *D*, Sequences of custom synthesized TSAD peptides aa242–268, aa242–256 and aa254-268. *E*, *In vitro* pull-down experiment using 10 μM of each SH3 domain and increasing amounts of TSAD aa242–268 (10, 20 and 40 μM) in a total volume of 100 μl. The GST-ITK-SH3 domain was added while attached to Glutathion Sepharose™ beads. In order to eliminate bead loss a 4 fold amount of GST-Glutathion Sepharose™ beads was added to the mixture, as is evidenced from the bottom panel. *F*, *In vitro* pull-down experiment performed as in *D*, using 10 μM of each SH3 domain, and 10 μM of the indicated TSAD peptides.

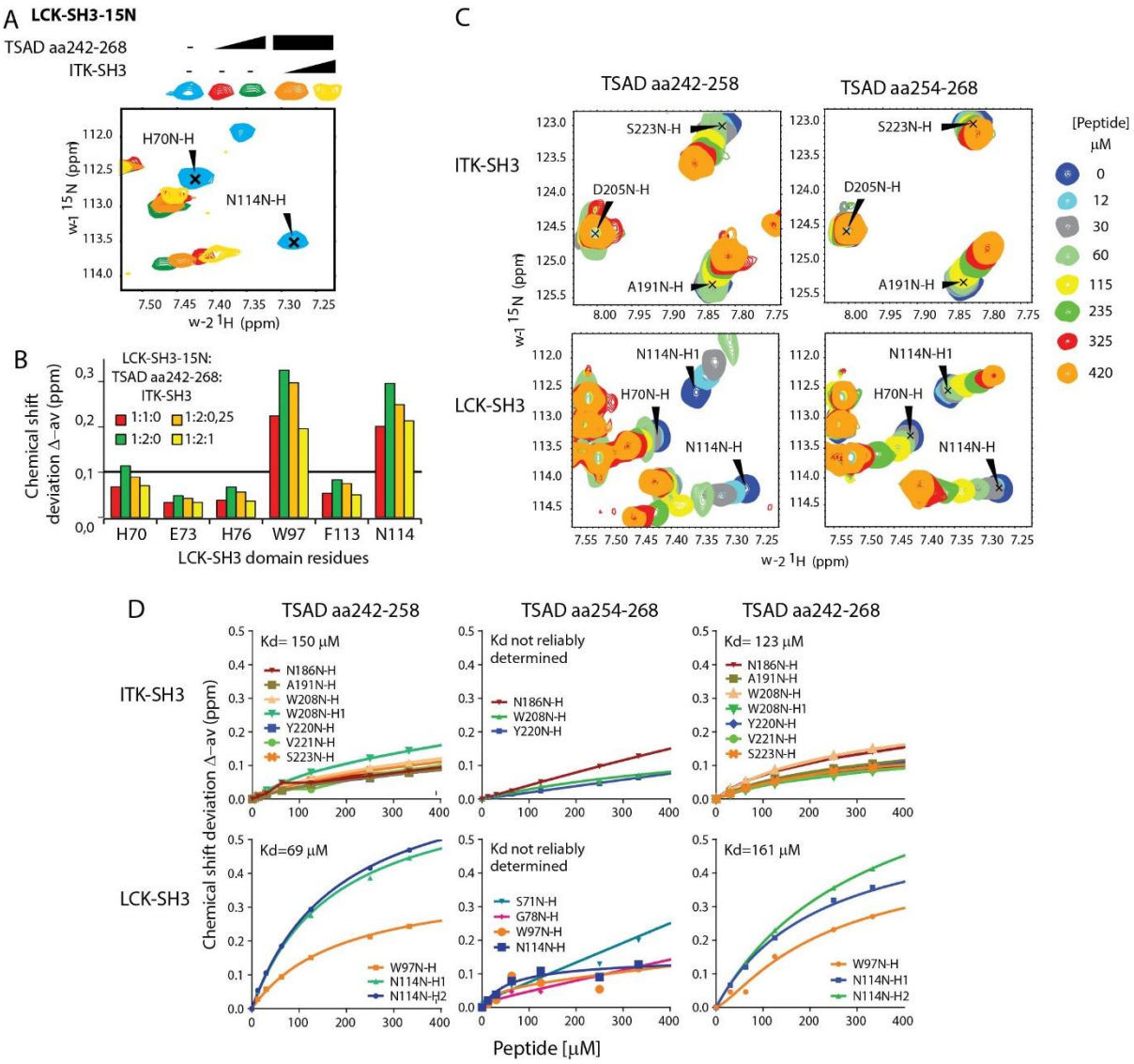

FIGURE 6. ITK SH3 competes with LCK SH3 for binding to TSAD aa242–268. *A*, Chemical shift deviations of selected residues in HSQC titration experiments performed with ^{15}N labeled LCK-SH3 (initially 0.25 mM) in the presence of increasing concentration of TSAD aa242–268 (red 0.25 mM and green 0.5 mM) followed by increasing amounts of non-labeled ITK SH3 (orange, yellow). *B*, Chemical shift deviations of selected LCK-residues from the HSQC experiment depicted in *A* (at 1:2:0,25 concentrations of LCK SH3, TSAD peptide and ITK SH3 were 0.2, 0.4 and 0.04 mM respectively, while at 1:2:1 the corresponding concentrations where 0.1, 0.2 and 0.1 mM). *C*, Chemical shift deviations of selected residues in HSQC titration experiments performed with ^{15}N labeled LCK-SH3 and ITK SH3 added to the same NMR tube in the presence of increasing concentration of TSAD aa242–258 or TSAD aa254-268 peptide. *D*, Titration curves for the indicated peptides based on HSQC shifts of selected amino acid signals from the indicated SH3 domains.

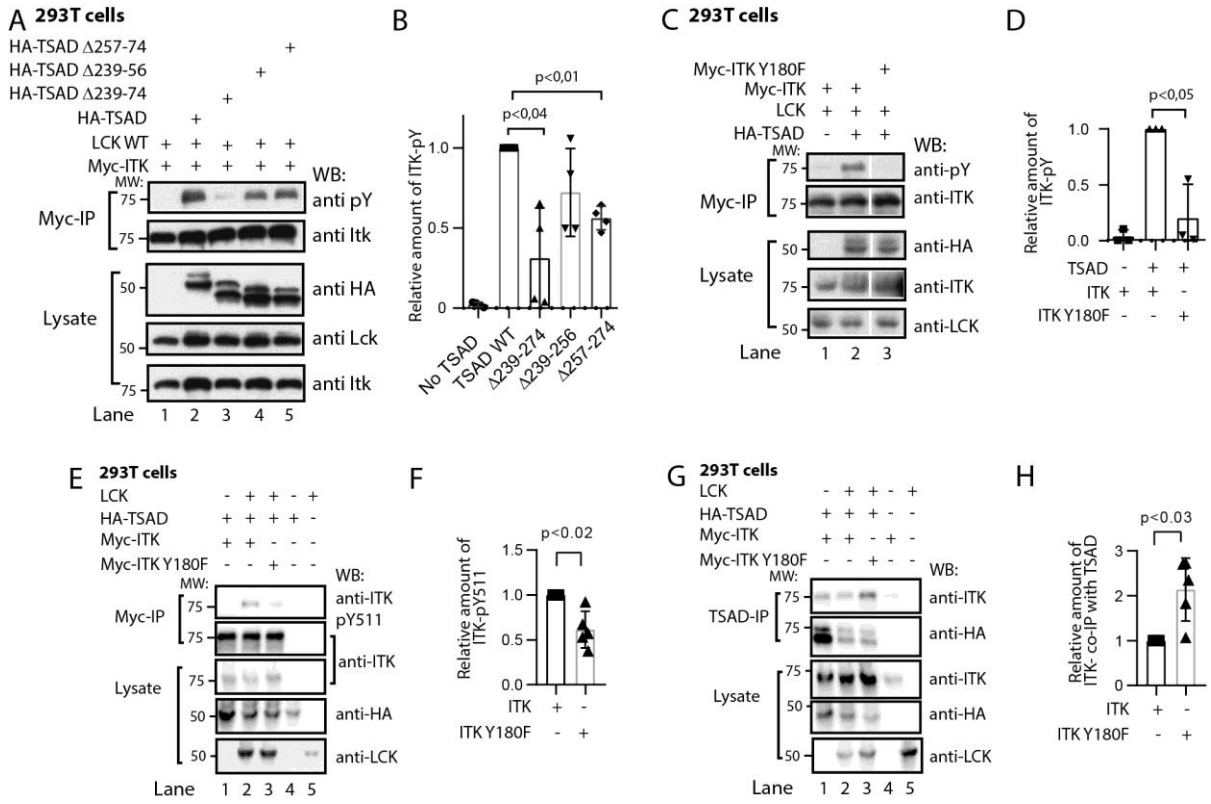

FIGURE 7. Association followed by dissociation of ITK to TSAD PRR is required for maximal phosphorylation of ITK in the presence of LCK. *A*, Immunoprecipitation experiment showing phosphorylation of ITK in the absence or presence of intact or mutated TSAD molecules. 293T cells were transfected with the indicated cDNA plasmids. Myc-tagged ITK proteins were immunoprecipitated from the cell lysates, and level of phosphorylation was assessed by immunoblotting. The result is one representative of two experiments. *B*, Graph shows quantitation of signal densities using ImageJ of the experiment shown in *A* (n=4, mean +-SD). *C* and *D*, Immunoprecipitation experiments as in *A* including also a myc-ITK-Y180F mutant (n=3, mean +-SD). *E-G*, Immunoprecipitation experiments in 293T cells expressing the indicated plasmids immunoblotted with the indicated antibodies. *F*, Graph shows quantitation of signal densities using ImageJ of the experiment shown in *E* and shows the relative amount of $pTyr^{511}$ signal where the $pTyr^{511}$ signal in ITK is set to 1 (n=5, mean +-SD). *H*, Graph shows quantitation of signal densities using ImageJ of the experiment shown in G and shows the relative amount ITK co-immunoprecipitated with TSAD (n=5, mean +-SD).

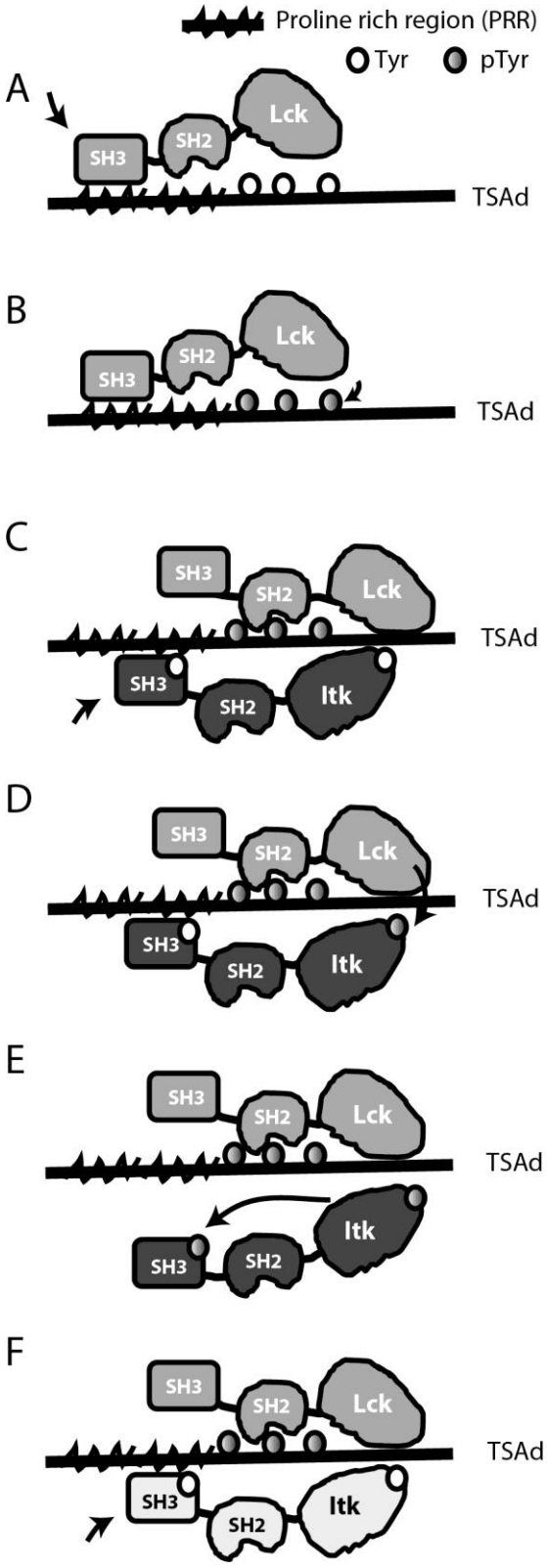

FIGURE 8. Schematic representation of TSAD-ITK-LCK interactions and their putative sequence. *A*, Open LCK binds to TSAD PRR and becomes activated. *B*, Active LCK phosphorylates the three TSAD C-terminal tyrosines. *C*, The LCK SH2 domain binds to TSAD pTyr, allowing LCK SH3 to detach from TSAD PRR. ITK binds to TSAD PRR. *D*, Active LCK phosphorylates ITK Tyr^{511}. *E*, Active ITK $pTyr^{511}$ autophosphorylates ITK Tyr^{180}. ITK $pTyr^{180}$ does not bind to TSAD PRR. *F*, Active LCK remains bound to TSAD pTyr. Next ITK molecule (indicated in different color) binds to TSAD PRR and process starts over from *D*.